Manipulating Topological Edge Spins in One-Dimensional Optical Lattice

Xiong-Jun Liu,[1, 2] Zheng-Xin Liu,[3, 4] and Meng Cheng[2]
[1]*Joint Quantum Institute, Department of Physics,*
University of Maryland, College Park, Maryland 20742, USA
[2]*Condensed Matter Theory Center, Department of Physics,*
University of Maryland, College Park, Maryland 20742, USA
[3]*Institute for Advanced Study, Tsinghua University, Beijing, 100084, P. R. China*
[4]*Department of Physics, Massachusetts Institute of Technology, Cambridge, Massachusetts 02139, USA*
(Dated: October 8, 2012)

We propose to observe and manipulate topological edge spins in 1D optical lattice based on currently available experimental platforms. Coupling the atomic spin states to a laser-induced periodic Zeeman field, the lattice system can be driven into a symmetry protected topological (SPT) phase, which belongs to the chiral unitary (AIII) class protected by $U(1)\times Z_2^T$ symmetry. In free-fermion case the SPT phase is classified by a Z invariant which reduces to Z_4 with interactions. The edge modes of the SPT phase are spin-polarized, with left and right edge spins polarized to opposite directions and forming a topological spin-qubit (TSQ). We demonstrate a novel scheme to manipulate the spin-polarized zero modes and realize quantum-tunneling driven spin Rabi-oscillations in a controllable manner. The manipulation of TSQs has potential applications to quantum computation.

PACS numbers: 71.10Pm, 37.10 Jk, 42.50.Ex, 71.70.Ej

arXiv:1209.2990v2 [cond-mat.mes-hall] 5 Oct 2012

Introduction.−Since the discovery of the quantum Hall effect in two-dimensional electron gas [1], the search for nontrivial topological states has become an exciting pursuit in condensed matter physics [2]. The recently observed time-reversal (TR) invariant topological insulators (TIs) have opened a new chapter in the study of topological phases (TPs), attracting great efforts in both theory and experiments [3, 4]. Depending on whether the ground states have long-range or short-range entanglement, the TPs can be classified into intrinsic or symmetry-protected topological (SPT) orders [5–7]. Unlike conventional quantum phases characterized by broken symmetries, TPs of quantum matter are classified by topological orders whose emergence does not break symmetry, and states of different topological orders cannot change into each other without closing the bulk gap. Being protected by the bulk gap, the intrinsic TPs are robust against any local perturbations, while the SPT phases are robust against those respecting given symmetries [5–8]. This property may be applied to the fault-tolerant quantum computation [9].

While the search of TR invariant TIs has been successful in solid-state systems, the recent great advancement in realizing effective spin-orbit (SO) interaction in cold atoms [10–15] opens intriguing new possibilities to probe SO effects [16] and TPs in a fully controllable fashion. Many theoretical proposals have been introduced in cold atoms for the study of TIs [17–21] and topological superfluids [22–25]. Experimental observations of these exotic phases are, however, delicate due to the demanding conditions such as complicated lattice configurations or SO interactions. By far the only experimentally realized SO interaction [11–15] is the equal Rashba-Dresselhaus-type SO term as theoretically proposed by Liu etal [10]. Therefore, to observe nontrivial topological states with currently available experimental platforms is particularly desired in the field of cold atoms [25].

In this letter, we propose to observe and manipulate topological edge spins in one-dimensional (1D) optical lattice with the SO interaction realizable in recent experiments [11–14]. The predicted SPT phase belongs to AIII class and is protected by $U(1)$ and chiral symmetries, with spin-polarized zero modes localized on boundaries. Our results not only provide a realistic platform to study SPT states in cold atoms, but also have broad range of applications including realizing single spin control in optical lattice, which is essential for spin-based quantum computation.

Model.−Our model is based on quasi-1D cold fermions trapped in an optical lattice, with the internal three-level Λ-type configuration coupled to radiation, as shown in Fig. 1. The transition $|g_\uparrow\rangle \to |e\rangle$ is induced by the laser field with Rabi-frequency $\Omega_1(x)=\Omega_0\sin(k_0x)$, and the one $|g_\downarrow\rangle \to |e\rangle$ is driven by another laser $\Omega_2(x)=\Omega_0\cos(k_0x)$. In the presence of a large one-photon detuning $|\Delta|\gg\Omega_0$ and a small two-photon detuning $|\delta|\ll\Omega_0$ for the transitions (Fig. 1(a)), the Hamiltonian of the light-atom coupling system reads $H=H_0+H_1$, with

$$\begin{aligned} H_0 &= \sum_{\sigma=\uparrow,\downarrow}\big[\frac{p_x^2}{2m}+V_\sigma(x)\big]|g_\sigma\rangle\langle g_\sigma| + \hbar\delta|g_\downarrow\rangle\langle g_\downarrow|, \\ H_1 &= \hbar\Delta|e\rangle\langle e| - \hbar\big(\Omega_1|e\rangle\langle g_\uparrow| + \Omega_2|e\rangle\langle g_\downarrow| + \text{H.c.}\big). \end{aligned}$$

Here the diagonal potentials $V_{\uparrow,\downarrow}(x)$ are used to construct the 1D optical lattice, and $\sigma_{y,z}$ are the Pauli matrices in spin space. For $|\Delta|\gg\Omega_0$, diagonalizing H_1 yields two nearly degenerate dressed states known as the dark and bright states given by [10] $|\chi_D\rangle=\cos(k_0x)|g_\uparrow\rangle-\sin(k_0x)|g_\downarrow\rangle$ and $|\chi_B\rangle=\sin(k_0x)|g_\uparrow\rangle+\cos(k_0x)|g_\downarrow\rangle$. Pro-

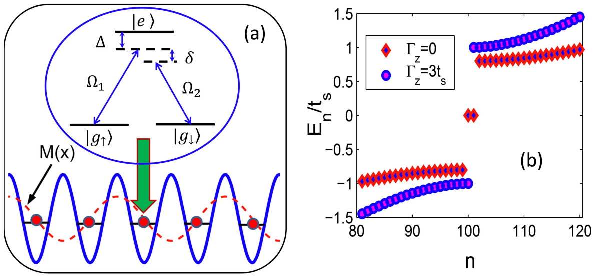

FIG. 1: (Color online) (a) Cold fermions trapped in 1D optical lattice with internal three-level Λ-type configuration coupled to radiation. (b) Energy spectra with open boundary condition in the topological (diamond, $\Gamma_z = 0$) and trivial (circle, $\Gamma_z = 3t_s$) phases. The SO coupled hopping $t_{\rm so}^{(0)} = 0.4t_s$.

jecting H onto the subspace of $|\chi_{B,D}\rangle$ gives rise to the equal Rashba-Dresselhaus-type SO interaction which has been predicted in theory [10], and remarkably realized in the recent experiments [11–15]. In this study, we shall work in the basis of hyperfine states $|g_{\uparrow,\downarrow}\rangle$. The effect of the small two-photon detuning is equivalent to a Zeeman field along z axis $\Gamma_z = \hbar\delta/2$, which in experiment can be precisely controlled with acoustic-optic modulator. Eliminating the excited state by $|e\rangle \approx \frac{1}{\Delta}(\Omega_1^*|g_\uparrow\rangle + \Omega_2^*|g_\downarrow\rangle)$ yields the effective Hamiltonian

$$\begin{aligned} H_{\rm eff} &= \frac{p_x^2}{2m} + \sum_{\sigma=1,2}\big[V_\sigma^{\rm Latt}(x) + \Gamma_z\sigma_z\big]|g_\sigma\rangle\langle g_\sigma| - \\ &\quad -\big[M(x)|g_\uparrow\rangle\langle g_\downarrow| + {\rm H.c.}\big], \qquad (1) \end{aligned}$$

where $M(x) = M_0\sin(2k_0x)$ with $M_0 = \frac{\hbar\Omega_0^2}{2\Delta}$ represents an additional laser-induced Zeeman field. To form a 1D lattice, we consider the optical dipole trapping potentials $V_\uparrow^{\rm Latt}(x) = V_\downarrow^{\rm Latt}(x) = -V_0\cos^2(2k_0x)$ with the lattice trapping frequency $\omega = (8V_0k_0^2/m)^{1/2}$ [26]. This effective model describes a system of spin-1/2 fermions experiencing a periodic transverse Zeeman field $M(x)$ which is commensurate with the 1D optical lattice [Fig. 1(a)].

We next derive the tight-binding model by taking that the fermions occupy the lowest s-orbitals $\phi_{s\sigma}$ ($\sigma =\uparrow,\downarrow$). From the even parity of $\phi_{s\sigma}$, one can verify that the periodic term $M(x)$ does not couple the intrasite orbitals $\phi_{s\uparrow}$ and $\phi_{s\downarrow}$, but leads to a spin-flip hopping given by $t_{\rm so}^{ij} = \int dx\phi_{s\uparrow}^{(i)}(x)M(x)\phi_{s\downarrow}^{(j)}(x)$, as a consequence of the induced SO interaction. The spin-conserved hopping is given by $t_s = \int dx\phi_{s\sigma}^{(j)}(x)\big[\frac{p_x^2}{2m} + V\big]\phi_{s\sigma}^{(j+1)}(x)$. Bearing these results in mind we write down the effective Hamiltonian in the tight-binding form: $H = -t_s\sum_{<i,j>,\sigma}\hat c_{i\sigma}^\dagger\hat c_{j\sigma} + \sum_i\Gamma_z(\hat n_{i\uparrow} - \hat n_{i\downarrow}) + \big[\sum_{<i,j>}t_{\rm so}^{ij}\hat c_{i\uparrow}^\dagger\hat c_{j\downarrow} + {\rm H.c.}\big]$, with $\hat n_{i\sigma} = \hat c_{i\sigma}^\dagger\hat c_{i\sigma}$. It can be verified that $t_{\rm so}^{j,j\pm1} = \pm(-1)^jt_{\rm so}^{(0)}$, where $t_{\rm so}^{(0)} = \frac{\Omega_0^2}{\Delta}\int dx\phi_s(x)\sin(2k_0x)\phi_s(x-a)$ with a the lattice constant. Redefining the spin-down operator $\hat c_{j\downarrow} \to e^{i\pi x_j/a}\hat c_{j\downarrow}$, we recast the Hamiltonian into

$$\begin{aligned} H &= -t_s\sum_{<i,j>}(\hat c_{i\uparrow}^\dagger\hat c_{j\uparrow} - \hat c_{i\downarrow}^\dagger\hat c_{j\downarrow}) + \sum_i\Gamma_z(\hat n_{i\uparrow} - \hat n_{i\downarrow}) + \\ &\quad +\Big[\sum_j t_{\rm so}^{(0)}(\hat c_{j\uparrow}^\dagger\hat c_{j+1\downarrow} - \hat c_{j\uparrow}^\dagger\hat c_{j-1\downarrow}) + {\rm H.c.}\Big]. \qquad (2) \end{aligned}$$

We analyze the symmetry of the above Hamiltonian. The TR and charge conjugation operators are respectively defined by $\mathcal{T} = iK\sigma_y$ with K the complex conjugation, and $\mathcal{C} : (\hat c_\sigma, \hat c_\sigma^\dagger) \longmapsto (\sigma_z)_{\sigma\sigma'}(\hat c_{\sigma'}^\dagger, \hat c_{\sigma'})$. One can check that while both $\mathcal{T}$ and $\mathcal{C}$ are broken in H, the chiral symmetry, defined as their product, is respected and $(\mathcal{CT})H(\mathcal{CT})^{-1} = H$, with $(\mathcal{CT})^2 = 1$. Note the chiral symmetry is still preserved if a Zeeman term $\Gamma_y\sigma_y$ along y axis is included in H. The complete symmetry group then reads $U(1)\times Z_2^T$, where $U(1)$ gives particle-number conservation and the anti-unitary group Z_2^T is formed by $\{I, \mathcal{CT}\}$. The SPT phase of our free-fermion system belongs to the chiral unitary (AIII) class and is characterized by a Z invariant [5–7]. The H can be rewritten in the k-space $H = -\sum_{k,\sigma\sigma'}\hat c_{k,\sigma}^\dagger[d_z(k)\sigma_z + d_y(k)\sigma_y]_{\sigma,\sigma'}\hat c_{k,\sigma'}$, with $d_y = 2t_{\rm so}^{(0)}\sin(ka)$ and $d_z = -\Gamma_z + 2t_s\cos(ka)$. This Hamiltonian describes a nontrivial topological insulator for $|\Gamma_z| < 2t_s$ and otherwise a trivial insulator, with the bulk gap $E_g = \min\{|2t_s - |\Gamma_z||, 2|t_{\rm so}^{(0)}|\}$ (Fig. 1 (b)). In particular, when $\Gamma_{y,z} = 0$ and $t_s = |t_{\rm so}^{(0)}|$, our model gives rise to a flat band with nontrivial topology.

Edge states.—The nontrivial topology can support degenerate boundary modes. Considering hard wall boundaries located at $x = 0, L$, respectively [27] and diagonalizing H in position space $H = \sum_{x_i}\mathcal{H}(x_i)$ with $\mathcal{H}(x_i) = -(t_s\sigma_z + it_{\rm so}^{(0)}\sigma_y)\hat c_{x_i}^\dagger\hat c_{x_i+a} + \Gamma_z\sigma_z\hat c_{x_i}^\dagger\hat c_{x_i} + h.c.$, we obtain the edge state localized on left boundary $x = 0$ as

$$\psi_L(x_i) = \frac{1}{\sqrt{\mathcal{N}}}[(\lambda_+)^{x_i/a} - (\lambda_-)^{x_i/a}]|\chi_+\rangle, \qquad (3)$$

and accordingly the one on $x = L$ by $\psi_R(x_i) = \frac{1}{\sqrt{\mathcal{N}}}[(\lambda_+)^{(L-x_i)/a} - (\lambda_-)^{(L-x_i)/a}]|\chi_-\rangle$. Here $\mathcal{N}$ is the normalization factor, $|\chi_\pm\rangle = [1, \pm1]^T$ are spin eigensates of σ_x, and $\lambda_\pm = (\Gamma_z \pm \sqrt{\Gamma_z^2 - 4t_s^2 + 4|t_{\rm so}^{(0)}|^2})/(2t_s + 2|t_{\rm so}^{(0)}|)$. Therefore the two edge states are polarized to the opposite $\pm x$ directions. Note the edge modes $\psi_{L,R}$ span the complete Hilbert space of *one single* 1/2-spin or spin-qubit. Each edge state equals *one-half* of a single spin, similar to the relation between a Majorana fermion and a complex fermion in topological superconductors. As a result, we expect the robustness of the zero modes to any local operations without breaking the $U(1)$ and $\mathcal{CT}$ symmetries. These properties of the topological spin qubit (TSQ) may be applicable to the fault-tolerant quantum computation [9]. Moreover, the Z classification implies that single-particle couplings respecting $U(1)$ and $\mathcal{CT}$ cannot gap out the edge modes in arbitrary N-chain system of 1D lattices, while, interestingly, we have confirmed that weak interactions can break Z down to Z_4 classification [28]. This result suggests an interesting platform to study classification of SPT phases with interactions.

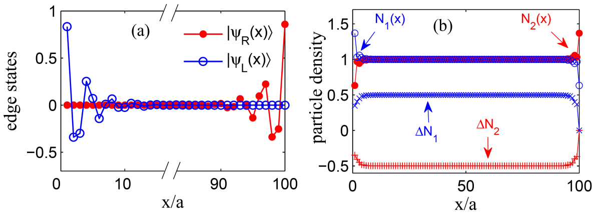

FIG. 2: (Color online) (a) Wave functions for zero modes $|\psi_{L,R}\rangle$; (b) 1/2-particle fractionalization (seen by $\Delta N_{1,2}$) for zero modes. The parameters $t_{\rm so}^{(0)}=0.4t_s$ and $\Gamma_z=0.3t_s$, with which the localization length of bound modes ξ_0=2.36a.

Existence of zero modes leads to particle fractionalization, which is another direct observable in experiment. A zero mode is contributed half from the valence band and half from the conduction band. Therefore, an edge state carries +1/2 (−1/2) particle if it is occupied (unoccupied) [28]. This result is confirmed by numerical simulation shown in Fig. 2, where we calculate $\Delta N_{1,2}(x_i)=\int_0^{x_i}dx' N_{1,2}(x')-x_i/a$ at half-filling, with $N_{1(2)}(x)$ the density of fermions when the left (right) edge mode is filled. The fermion number carried by an occupied (unoccupied) edge mode is then given by $n_{1(2)}=\Delta N_{1(2)}(\xi)$ with $\xi\gg\xi_0$. Here $\xi_0=-a/\ln|\lambda_+|$ is the localization length of $\psi_{L,R}$. The 1/2-fractionalization is clearly seen when ξ is several times greater than ξ_0 (Fig. 2 (b)). Being a topological invariant, the 1/2-fractionalization can be confirmed to be robust against weak disorder scatterings without breaking the given symmetries.

Correlation effects.—A particular advantage in cold atoms is that one can investigate correlation effects on the predicted SPT phase by precisely controlling the interaction. For spin-1/2 cold fermions the onsite Hubbard interaction $U\sum_i n_{i\uparrow}n_{i\downarrow}$ can be well controlled by Feshbach resonance [26]. We adopt here the Abelian bosonization approach combined with renormalization group (RG) analysis to probe interaction effects in single-chain system at critical point. With low energy approximation we linearize the fermion dispersion near Fermi points $k_F=\frac{\pi}{2a}$ by $\hat{c}_s(x)\approx\sum_{r,s=\pm1}\psi_{rs}e^{irk_Fx}$, where r/s is the chiral/spin index. Using the standard bosonization formula [29]: $\psi_{rs}=\frac{1}{\sqrt{2\pi a}}e^{-\frac{i}{\sqrt{2}}[r\phi_\rho-\theta_\rho+s(r\phi_\sigma-\theta_\sigma)]}$, we reach the bosonized Hamiltonian density $\mathcal{H}=\sum_{\nu=\rho,\sigma}\mathcal{H}_\nu+\mathcal{H}_1$ with $\mathcal{H}_\nu=\frac{v_\nu}{2}[K_\nu(\partial_x\theta_\nu)^2+K_\nu^{-1}(\partial_x\phi_\nu)^2]+\frac{2g_\nu}{(2\pi a)^2}\cos2\sqrt{2}\phi_\nu$ and $\mathcal{H}_1=\frac{u}{\pi a}\sin\sqrt{2}\phi_\rho\cos\sqrt{2}\theta_\sigma+\frac{w}{\pi a}\cos\sqrt{2}\phi_\rho\sin\sqrt{2}\theta_\sigma$. Here $g_{\rho,\sigma}$ arise from umklapp scattering and spin backscattering, respectively. The bare values are $v_\nu=v_FK_\nu, g_\rho=-g_\sigma=U, u=2t_{\rm so}^{(0)}, w=\Gamma_y$ in units of t_s. At half-filling $\mathcal{H}$ respects $\mathbb{O}(4)\cong\mathbb{SU}(2)\times\mathbb{SU}(2)$ symmetry if $u=w=0$ [30]. For $U>0$, the umklapp scattering term $\cos2\sqrt{2}\phi_\rho$ drives the system into a Mott insulating phase with a charge gap. The spin sector remains at the fixed point with $K_\sigma^*=1$, described by $\mathbb{SU}(2)_1$ Wess-Zumino-Witten model [31]. When $u,w\neq0$, such symmetry is reduced to the $\mathbb{U}(1)$ subgroup.

For the large-U limit, the charge boson ϕ_ρ is pinned to its classical minima $\cos2\sqrt{2}\phi_\rho=1$, and the system is a Mott insulator, regardless of the mass terms. In the weak-coupling regime, the interaction effects on the phase boundary can be studied with RG method up to one-loop order [2]. The RG flow equations for the coupling constants u,v,g_ρ,g_σ are given by [28]:

$$\begin{aligned}\frac{\mathrm{d}u}{\mathrm{d}l}&=\frac{3-K_\rho}{2}u-\frac{g_\rho u}{4\pi v_F}+\frac{g_\sigma u}{4\pi v_F},\\ \frac{\mathrm{d}w}{\mathrm{d}l}&=\frac{3-K_\rho}{2}w+\frac{g_\rho w}{4\pi v_F}+\frac{g_\sigma w}{4\pi v_F},\\ \frac{\mathrm{d}g_\rho}{\mathrm{d}l}&=\frac{g_\rho^2}{\pi v_F},\quad\frac{\mathrm{d}g_\sigma}{\mathrm{d}l}=\frac{g_\sigma^2}{\pi v_F}.\end{aligned}\tag{4}$$

Here l is the logarithm of the length scale. The renormalization of Luttinger parameters K_ν has been neglected as it is a higher order correction. For $U>0$, g_σ marginally flows to zero so we drop it off below. g_ρ is marginally relevant and can be solved by $g_\rho(l)=\frac{\pi v_Fg_\rho(0)}{\pi v_F-g_\rho(0)l}$. Substituting this result into RG equations of u and w yields after integration $u(l)=u(0)[1-\frac{g_\rho(0)l}{\pi v_F}]^{\frac14}e^{(3-K_\rho)l/2}, w(l)=w(0)[1+\frac{g_\rho(0)l}{\pi v_F}]^{\frac14}e^{(3-K_\rho)l/2}$. The physics is clear: the repulsive interaction ($g_\rho>0$) suppresses SO induced mass term u while enhances the trivial mass term w. The fate of the system depends on which of u and w reaches the strong-coupling regime first. Assuming $|g_\rho(0)l|\ll v_F$, we find the TP transition occurs at

$$u(0)=\big[w(0)\big]^\gamma,\ \gamma\approx1-\frac{g_\rho(0)}{4\pi v_F(3-K_\rho)}.\tag{5}$$

This gives the scaling law at the phase boundary with interaction. Note $\gamma<1$ for $U>0$. The above scaling relation implies that a repulsive interaction suppresses the SPT phase. Accordingly, if initially the noninteracting system is topologically nontrivial with $u(0)>w(0)>0$, increasing U to the regime $u(0)<[w(0)]^\gamma$ drives the system into a trivial phase.

Single spin control.—Now we study an interesting application of the present results to realizing single spin control. Besides the edge modes localized on the ends, TSQs can also be obtained in the middle areas by creating mass domains in the lattice. This can be achieved by applying a local Zeeman term Γ_y or Γ_z. For example, we consider $\Gamma_z=0$ everywhere, but $\Gamma_y=\Gamma_0$ for $x_1<x<x_2$ and $\Gamma_y=0$ otherwise. The local Γ_y can be generated by applying another two lasers which cross with the 1D lattice and couple the atoms in the area $x_1<x<x_2$ to induce a local resonant Raman coupling between $|g_\uparrow\rangle$ and $|g_\downarrow\rangle$ (Fig. 3(a)). Employing a $\pi/2$-phase offset in the Rabi-frequencies of the two lasers, the Raman coupling takes the form $\Gamma_0\sigma_y$, with Γ_0 controlled

by the laser strength. When $|\Gamma_0| > 2|t_{\rm so}^{(0)}|$ a mass domain is created, associated with two midgap spin states $|\psi_\pm\rangle$ respectively localized around $x = x_{1,2}$ (Fig. 3(a)). The width $\Delta x = x_2 - x_1$ and height of the domain are respectively adjusted by the waist size and strength of the two laser beams. Due to the nonlocality of the TSQ, creation of a single qubit here is not restricted by the size of the laser beams. This is a fundamental difference from creating conventional single qubit by optical dipole trapping which requires tiny-sized laser beams to reach a very small trapping volume [33]. Note in realistic case the laser induced Γ_y may vary fast but not in the form of step functions around $x = x_{1,2}$, which, however, does not affect the main results presented here. Coupling between $|\psi_+\rangle$ and $|\psi_-\rangle$ results in an energy splitting $2\mathcal{E} \propto e^{-(|\Gamma_0|-2|t_{\rm so}^{(0)}|)\Delta x/(2at_s)}$, which is controlled by Γ_0 and Δx (Fig. 3(a), lower panel). In the limit $(|\Gamma_0| - 2|t_{\rm so}^{(0)}|)\Delta x/(2at_s) \gg 1$, such coupling is negligible, and the two zero modes consist of a single spin qubit which is topologically stable. Let $|\psi_+\rangle$ be initially occupied while $|\psi_-\rangle$ be left vacancy. Reducing $|\Gamma_0|$ smoothly can open the coupling in $|\psi_\pm\rangle$ and lead to spin state evolving as [34] $|\psi(t)\rangle = \alpha(t)\varphi_-(x - x_1)|\chi_-\rangle + \beta(t)\varphi_+(x - x_2)|\chi_+\rangle$, with $\alpha(0) = 0, \beta(0) = 1$, and $\varphi_\pm$ the spatial parts of the bound state wave-functions. The spin-polarization densities are given by $s_{x,y,z}(x,t) = \langle\psi(x)|\sigma_{x,y,z}|\psi(x)\rangle$, and the spin expectation values $S_{x,y,z}(t) = \int dx s_{x,y,z}(x,t)$. It can be verified that $S_y(t) = 0$, and

$$\begin{aligned} S_x(t) &= |\alpha(t)|^2 - |\beta(t)|^2, \\ S_z(t) &= 2\mathrm{Re}\big[\alpha(t)\beta^*(t)\int dx\varphi_+^*(x)\varphi_-(x)\big]. \end{aligned} \tag{6}$$

This phenomenon is analogous to spin precession with the rotating angle yielding $\gamma(t) = 2\int_0^t dt'\mathcal{E}(t')$. We have then $\alpha = \cos\gamma(t)$ and $\beta = \sin\gamma(t)$. The amplitude of $S_z(t)$ is given by $S_z^{\max} = |\int dx\varphi_+^*(x)\varphi_-(x)|$, which measures the overlapping integral of $\varphi_\pm$. Accordingly, if we apply the local Zeeman field along z rather than y axis, we shall obtain that the spin evolves in the x-y plane. Note the spin Rabi-oscillation is induced by quantum tunneling. Therefore it is associated with a tunneling current given by $J_m(t) = -\frac{\Delta x\mathcal{E}}{2\pi\hbar}\partial_t|\alpha(t)|^2$ between x_1 and x_2. In experiment the internal states of a single atom can be detected without energy transfer [35], which is applicable to observe the spin Rabi-oscillations, while the oscillation of $S_x(t)$ can be more conveniently observed by measuring the number of fermions $\langle n_\pm(t)\rangle$ localized on $x_{1,2}$, and $J_m(t)$ can be detected by measuring the change rate with time of such fermion numbers.

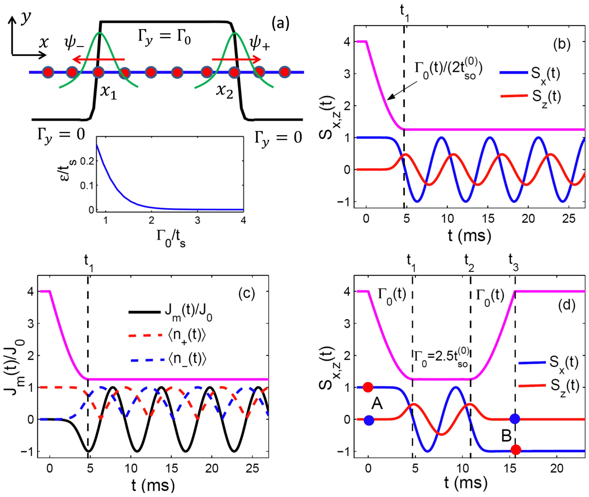

FIG. 3: (Color online) Spin Rabi-oscillations with the parameters $t_s = 3.15$kHz, $t_{\rm so}^{(0)} = 0.4t_s$, and $\Delta x = 10a \sim 4\mu m$. (a) Mass domain created by setting $|\Gamma_0| > 2t_{\rm so}^{(0)}$ for $x_1 < x < x_2$ which localizes a spin-qubit composed of two bound modes $|\psi_\pm\rangle$ on $x = x_1, x_2$, respectively; (b) Spin Rabi-oscillation by smoothly reducing $|\Gamma_0|$ from $8t_{\rm so}^{(0)}$ to $2.5t_{\rm so}^{(0)}$; (c) The mass current $J_m(t)$ and expectation values of particle numbers $\langle n_\pm(t)\rangle$ in states $|\psi_\pm\rangle$; (d) Spin-flip operation by controlling that $\gamma(t_3) = (2m+1)\pi$ with $m = 1$. The initial spin state $|\chi_+\rangle$ (Points A) flips to be $|\chi_-\rangle$ (Points B).

We show in Fig. 3 (b-d) the numerical simulation for single spin control with the parameter regime that $t_s = 3.15$kHz, $t_{\rm so}^{(0)} = 0.4t_s$, and $\Delta x = 10a$. For $t < 0$, $\Gamma_0 = 8t_{\rm so}^{(0)}$ and the coupling in $|\psi_\pm\rangle$ is negligible. Reducing Γ_0 at $t > 0$ leads to spin evolution and by fixing $\Gamma_0 = 2.5t_{\rm so}^{(0)}$ for $t > t_1$ the spin oscillates with a period of 5.984ms (b-c). Note the quantum state of the spin can be precisely controlled by properly manipulating $\gamma(t)$. For example, in Fig. 3 (d) we demonstrate the spin-flip operation $|\chi_+\rangle \to |\chi_-\rangle$ by requiring $\gamma(t_3) = (2m+1)\pi$. Here $m \in Z$ and in (d) we take $m = 1$. Note one may integrate multiple TSQs with e.g. atom-chip technology and individually control them by creating multiple mass domains in the 1D lattice. The precise manipulation of such integrated TSQs may have interesting applications in developing scalable spin-based quantum computers.

Before conclusion we estimate the parameter values for realistic experimental observations. For example, in ^{40}K atoms we have the recoil energy $E_R/\hbar = \hbar k^2/2m = 48$kHz using red-detuned lasers of wavelength 780nm to form the optical lattice. Taking that $V_0 = 5E_R$ and $M_0 = 2E_R$, we have that the lattice trapping frequency $\omega = 214$kHz, and hopping coefficients $t_s/\hbar \simeq 3.15$kHz and $t_{\rm so}^{(0)}/\hbar \simeq 1.3$kHz. Then the bulk gap equals $E_g/\hbar = 2.6$kHz for $\Gamma_z = 0$, indicating a temperature $T = 19$nK for the experimental observation.

Conclusions.—In conclusion, we have proposed to observe and manipulate the topological edge spins in 1D optical lattice with currently available experimental platforms. In the free-fermion case the SPT phase belongs to the AIII class characterized by a Z invariant which breaks down to Z_4 with interactions. The spin-polarized zero edge modes in the nontrivial SPT phase form TSQs. Our results are of broad range of interests and applications including the manipulation of TSQs which may be applicable in developing spin-based quantum computers.

We thank X. G. Wen, X. Chen, Vincent W. Liu, and Cenke Xu for helpful discussions. We acknowledge the support from JQI-NSF-PFC, Microsoft-Q, and DARPA-QuEST.

[1] K.V. Klitzing, G. Dorda, and M. Pepper, Phys. Rev. Lett. **45**, 494 (1980); D. C. Tsui and H. L. Stormer and A. C. Gossard, Phys. Rev. Lett. **48**, 1559 (1982).
[2] F. D. M. Haldane, Phys. Rev. Lett. **50**, 1153 (1983); Phys. Lett. **93**, 464 (1983); N. Read and D. Green, Phys. Rev. B **61**, 10267 (2000); A. Y. Kitaev, Physics-Uspekhi **44**, 131 (2001).
[3] C. L. Kane and E. J. Mele, Phys. Rev. Lett. **95**, 146802 (2005); B. A. Bernevig, T. L. Hughes and S. -C. Zhang, Science, **314** 1757 (2006); L. Fu, C. L. Kane, and E. J. Mele, Phys. Rev. Lett. **98**, 106803 (2007); J. E. Moore and L. Balents, Phys. Rev. B **75**, 121306 (R) (2007); R. Roy, *ibid* **79**, 195322 (2009).
[4] M. Z. Hasan and C. L. Kane, Rev. Mod. Phys. **82**, 3045 (2010); X. -L. Qi and S. -C. Zhang, *ibid* **83**, 1057 (2011).
[5] A. Altland and Martin R. Zirnbauer, Phys. Rev. B **55**, 1142 (1997).
[6] Z. C. Gu and X. G. Wen, Phys. Rev. B **80**, 155131 (2009); X. Chen, Z. -C. Gu, and X. -G. Wen, *ibid* **82**, 155138 (2010); X. -G. Wen, *ibid* **85**, 085103 (2012).
[7] Shinsei Ryu, Andreas Schnyder, Akira Furusaki, Andreas Ludwig, New J. Phys. **12**, 065010 (2010).
[8] L. Fidkowski and A. Kitaev, Phys. Rev. B **81**, 134509 (2010),; A. M. Turner, F. Pollmann, and E. Berg, *ibid* **83**, 075102 (2011); L. Fidkowski and A. Kitaev, *ibid* **83**, 075103 (2011).
[9] Y. Kitaev, Ann. Phys. 303, 2 (2003); S. Das Sarma, M. Freedman, and C. Nayak, Phys. Rev. Lett. 94, 166802 (2005); C. Nayak et al., Rev. Mod. Phys. **80**, 1083 (2008).
[10] X. -J. Liu, M. F. Borunda, X. Liu, and J. Sinova, Phys. Rev. Lett. **102**, 046402 (2009).
[11] Y.-J. Lin, K. Jiménez-García, and I. B. Spielman, Nature **471**, 83 (2011).
[12] M. Chapman and C. Sá de Melo, Nature **471**, 41 (2011).
[13] P. Wang et al., Phys. Rev. Lett. **109**, 095301 (2012).
[14] L. W. Cheuk, A. T. Sommer, Z. Hadzibabic, T. Yefsah, W. S. Bakr, and M. W. Zwierlein, Phys. Rev. Lett. **109**, 095302 (2012).
[15] Jin-Yi Zhang et al., Phys. Rev. Lett. **109**, 115301 (2002).
[16] J. Larson, J.-P. Martikainen, A. Collin, E. Sjoqvist, Phys. Rev. A **82**, 043620 (2010); D. Sokolovski, E. Ya. Sherman, *ibid* **84**, 030101(R) (2011); J. D. Sau, R. Sensarma, S. Powell, I. B. Spielman, S. Das Sarma, Phys. Rev. B **83**, 140510(R) (2011); T. Ozawa, G. Baym, Phys. Rev. Lett. **109**, 025301 (2012); G. I. Martone, Y. Li, L. P. Pitaevskii, S. Stringari, arXiv:1207.6804 (2012).
[17] X. -J. Liu, X. Liu, L. C. Kwek and C. H. Oh, Phys. Rev. Lett. **98**, 026602 (2007); Phys. Rev. B **79**, 165301 (2009).
[18] C. Wu, Phys. Rev. Lett. **101**, 186807 (2008); X.-J. Liu, X. Liu, C. Wu, and J. Sinova, Phys. Rev. A **81**, 033622 (2010); Y. Yu, K. Yang, Phys. Rev. Lett. **105**, 150605 (2010).
[19] N. Goldman, I. Satija, P. Nikolic, A. Bermudez, M.A. Martin-Delgado, M. Lewenstein, I. B. Spielman, Phys. Rev. Lett. **105**, 255302 (2010); N. Goldman, J. Beugnon, and F. Gerbier, *ibid* **108**, 255303 (2012).
[20] X. Li, E. Zhao, and W. V. Liu, arXiv:1205.0254 (2012).
[21] G. Liu, S. -L. Zhu, S. Jiang, F. Sun, and W. M. Liu, Phys. Rev. A **82**, 053605 (2010); F. Mei, S. -L. Zhu, Z. -M. Zhang, C. H. Oh, N. Goldman, *ibid* **85**, 013638 (2012).
[22] C. Zhang, S. Tewari, R. Lutchyn, and S. Das Sarma, Phys. Rev. Lett. **101**, 160401 (2008); Y. Zhang, L. Mao, C. Zhang, *ibid* **108**, 035302 (2012).
[23] M.Sato, Y. Takahashi, S. Fujimoto, Phys. Rev. Lett. 103 020401 (2009).
[24] S. -L. Zhu, L. B. Shao, Z. D. Wang, Lu-Ming Duan, Phys. Rev. Lett. **106**, 100404 (2011); L. He, X. -G. Huang, *ibid* **108**, 145302 (2012); Phys. Rev. B **86**, 014511 (2012).
[25] Kangjun Seo, Li Han, and C. A. R. Sá de Melo, Phys. Rev. Lett. **109**, 105303 (2012).
[26] I. Bloch, J. Dalibard, and W. Zwerger, Rev. Mod. Phys. **80**, 885 (2008).
[27] T. P. Meyrath, F. Schreck, J. L. Hanssen, C.-S. Chuu, and M. G. Raizen, Phys. Rev. A **71**, 041604(R) (2005).
[28] See Supplementary Material for more details.
[29] T. Giamarchi, Quantum physics in one dimension (Oxford University Press, 2004).
[30] C. N. Yang, Phys. Rev. Lett. **63**, 2144 (1996); C. N. Yang and S. C. Zhang, Mod. Phys. Lett. **B4**, 759 (1990).
[31] A. O. Gogolin, A. A. Nersesyan, and A. M. Tsvelik, Bosonization and Strongly Correlated Systems (Cambridge University Press, 1998).
[32] L. Balents and M. P. A. Fisher, Phys. Rev. B **53**, 12133 (1996).
[33] N. Schlosser, G. Reymond, I. Protsenko, and P. Grangier, Nature, **411**, 1024 (2001).
[34] We neglect the couplings between $|\psi_\pm\rangle$ and bulk states $|u_k\rangle$, which is valid when $|\langle\psi_\pm|\partial_t|u_k\rangle| \ll E_g$ during the manipulation.
[35] J. Volz, R. Gehr, G. Dubois, J. Estève, and J. Reichel, Nature **475**, 210 (2011).

Manipulating Topological Edge Spins in One-Dimensional Optical Lattice — Supplementary Material

In this supplementary material we provide the details of some results in the main text.

Appendix A: Topological Classification

1. Noninteracting regime

With the inclusion of both Γ_y and Γ_z, the generic Hamiltonian obtained in the main text is given by

$$\begin{aligned} H &= -\sum_j \left[t_s(\hat{c}^\dagger_{j\uparrow}\hat{c}_{j+1\uparrow} - \hat{c}^\dagger_{j\downarrow}\hat{c}_{j+1\downarrow}) - t^{(0)}_{\mathrm{so}}(\hat{c}^\dagger_{j\uparrow}\hat{c}_{j+1\downarrow} - \hat{c}^\dagger_{j\uparrow}\hat{c}_{j-1\downarrow}) + \mathrm{H.c.}\right] + \sum_j \left[\Gamma_z(\hat{n}_{j\uparrow} - \hat{n}_{j\downarrow}) - \Gamma_y(i\hat{c}^\dagger_{j\uparrow}c_{j\downarrow} + \mathrm{H.c.})\right] \\ &= \sum_{k,\sigma} \hat{c}^\dagger_{k,\sigma\sigma'}\mathcal{H}_{\sigma\sigma'}(k)\hat{c}_{k,\sigma'}, \end{aligned} \tag{A1}$$

where $\mathcal{H}(k) = d_y(k)\sigma_y + d_z(k)\sigma_z$ with $d_y = \Gamma_y + 2t^{(0)}_{\mathrm{so}}\sin(ka)$ and $d_z = \Gamma_z - 2t_s\cos(ka)$. The full symmetry of the system is $U(1) \times (CT)$, where the phase transformation operator $U(1)$, charge conjugation operator C and time reversal operator T are defined as:

$$\begin{aligned} &U(\theta)\hat{c}U(\theta)^{-1} = e^{i\theta}\hat{c}, \qquad \mathcal{C}\hat{c}\mathcal{C}^{-1} = \sigma_z\hat{c}^\dagger; \\ &\mathcal{T}\hat{c}\mathcal{T}^{-1} = -i\sigma_y K\hat{c}, \quad (\mathcal{C}\mathcal{T})\hat{c}(\mathcal{C}\mathcal{T})^{-1} = \sigma_x\hat{c}^\dagger. \end{aligned}$$

The following commutation relations can be checked: $\mathcal{C}^2 = -\mathcal{T}^2 = (\mathcal{C}\mathcal{T})^2 = 1, \{\mathcal{C},\mathcal{T}\} = 0$, and $[\mathcal{C}\mathcal{T}, U(1)] = 0$. The subgroup $\{I, \mathcal{C}\mathcal{T}\}$ is anti-unitary and can be denoted as Z_2^T, and the complete symmetry group can also be written as $U(1) \times Z_2^T$. Owning to this symmetry group, the free fermion system belongs to chiral unitary (AIII) class and is characterized by a Z invariant in the noninteracting case.

If the Zeeman field along y axis vanishes, i.e. $\Gamma_y = 0$, alternatively the symmetry group can be chosen as $U(1) \rtimes \times (C \times T)$ where $U(\theta)\hat{c}U(\theta)^{-1} = e^{i\theta}\hat{c}$, $\mathcal{C}\hat{c}\mathcal{C}^{-1} = \sigma_x\hat{c}^\dagger$, $\mathcal{T}\hat{c}\mathcal{T}^{-1} = K\hat{c}$, with $\mathcal{C}^2 = \mathcal{T}^2 = (\mathcal{C}\mathcal{T})^2 = 1$, and $[\mathcal{C},\mathcal{T}] = 1, \mathcal{T}U(\theta) = U(-\theta)\mathcal{T}, \mathcal{C}U(\theta) = U(-\theta)\mathcal{C}$. In this case both T and C are symmetries of the Hamiltonian and the system then belongs to the BDI class which is also classified by a Z invariant in the non-interacting case.

2. Interacting regime

For a N-chain system under the half-filling condition, the total ground-state degeneracy is C^N_{2N} without interactions. Let $\hat{c}_{m,L/R}$ and $\hat{c}^\dagger_{m,L/R}$ be the annihilation and creation operators of the left/right edge mode for the m-th chain, respectively, where $\hat{c}_L = (\hat{c}_\uparrow + \hat{c}_\downarrow)/\sqrt{2}$ and $\hat{c}_R = (\hat{c}_\uparrow - \hat{c}_\downarrow)/\sqrt{2}$. The edge states of the m-th chain can be written as $\hat{c}^\dagger_{m,L}|0\rangle_m$ and $c^\dagger_{m,R}|0\rangle_m$, where $|0\rangle_m$ is the ground state for the bulk.

An interesting question is what happens if we turn on interactions. It turns out that in the presence of interactions, the Z classification breaks down to Z_4. To confirm this result, we will study the ground states of a N-chain system step by step.

First, for $N = 2$, a generic $U(1) \times (CT)$-symmetric interaction between the edge zero modes reads

$$\begin{aligned} H_{12} &= \sum_{s=L,R} \left[V^{(4)}_{12}\hat{c}^\dagger_{1,s}\hat{c}_{1,s}\hat{c}^\dagger_{2,s}\hat{c}_{2,s} + (V^{(4)}_{12})^*\hat{c}_{1,s}\hat{c}^\dagger_{1,s}\hat{c}_{2,s}\hat{c}^\dagger_{2,s}\right] \\ &= \sum_s V^{(4)}_{12}(2\hat{c}^\dagger_{1,s}\hat{c}_{1,s}\hat{c}^\dagger_{2,s}\hat{c}_{2,s} - \hat{c}^\dagger_{1,s}\hat{c}_{1,s} - \hat{c}^\dagger_{2,s}\hat{c}_{2,s} + 1). \end{aligned} \tag{A2}$$

With above interaction the minimum degeneracy of the 2-chain system is two-fold, which is obtained when $V^{(4)}_{12} = (V^{(4)}_{12})^* = -V_0 < 0$. It is straightforward to check that the states $|01\rangle_1|01\rangle_2$ and $|10\rangle_1|10\rangle_2$ have energy $-2V_0$ while the states $|10\rangle_1|01\rangle_2$, $|01\rangle_1|10\rangle_2$,$|00\rangle_1|11\rangle_2$, and $|11\rangle_1|00\rangle_2$ have a higher energy 0. Then the ground state is two-fold degenerate, as given by $|01\rangle_1|01\rangle_2$ and $|10\rangle_1|10\rangle_2$.

Second, for $N=3$, the ground state degeneracy $C_6^3=20$ can be reduced to 2 by two-chain interactions according to (A2): $H_{\rm int}=H_{12}+H_{23}$. For instance, if $V_{12}^{(4)}=V_{23}^{(4)}=-V_0<0$, the two-fold degenerate ground states are

$$|01\rangle_1|01\rangle_2|01\rangle_3,\quad |10\rangle_1|10\rangle_2|10\rangle_3; \tag{A3}$$

and if $V_{12}=-V_{23}=-V_0<0$, the ground states read

$$|01\rangle_1|01\rangle_2|10\rangle_3,\quad |10\rangle_1|10\rangle_2|01\rangle_3. \tag{A4}$$

However, for the 3-chain system, one should also consider three-body interactions. One of the possible 3-chain interactions reads

$$H_{123}=\sum_s(V_{123}^{(6)}\hat{c}_{1,s}^\dagger\hat{c}_{1,s}\hat{c}_{2,s}^\dagger\hat{c}_{2,s}\hat{c}_{3,s}^\dagger\hat{c}_{3,s}+V_{123}^{(6)}\hat{c}_{1,s}\hat{c}_{1,s}^\dagger\hat{c}_{2,s}\hat{c}_{2,s}^\dagger\hat{c}_{3,s}\hat{c}_{3,s}^\dagger), \tag{A5}$$

where $V_{123}^{(6)}=(V_{123}^{(6)})^*$. It is straightforward to see that above interaction is identical to a summation of two-body interactions and can not split the degeneracy of the ground states. Other possible 3-chain interactions include

$$\begin{aligned} H_{123}' &= \sum_s V_{123}^{(4)}\left[\left(c_{1,s}^\dagger c_{2,s}^\dagger c_{2,s}c_{3,s}+c_{1,s}c_{2,s}c_{2,s}^\dagger c_{3,s}^\dagger\right)+\text{h.c.}\right] && \text{(A6)}\\ &= V_{123}^{(4)}(2c_{2,s}^\dagger c_{2,s}-1)(c_{1,s}^\dagger c_{3,s}+c_{3,s}^\dagger c_{1,s}), && \text{(A7)}\end{aligned}$$

It can be easily checked that in the case (A3) the perturbation H_{123}' have zero matrix elements in the ground-state subspace and hence can not spilt the degeneracy. The condition is similar in another case (A4). The difference is that, in case (A4), H_{123}' mixes the ground states with higher energy states. For instance, the state $|01\rangle_1|01\rangle_2|10\rangle_3$ is mixed with $|11\rangle_1|01\rangle_2|00\rangle_3$ to lower its energy. At the same time the state $|10\rangle_1|10\rangle_2|01\rangle_3$ is mixed with $|00\rangle_1|10\rangle_2|11\rangle_3$ to lower the energy with the same amount. As a result, the two new states, as the new ground states, are still degenerate. Therefore, the topological properties of 3 chains are stable against interactions respecting the symmetry, and we need to investigate the 4-chain system.

Finally, for $N=4$, it turns out that we can find a path to smoothly reduce the ground state degeneracy to 1. It is easy to verify that degeneracy of the ground states can be reduced to 4 under two-body interaction $H_{\rm int}=H_{12}+H_{23}+H_{34}$ with $V_{12}=-V_{23}=V_{34}=-V_0<0$. These four ground states are given by

$$\begin{aligned}&|01\rangle_1|01\rangle_2|10\rangle_3|10\rangle_4,\quad |10\rangle_1|10\rangle_2|01\rangle_3|01\rangle_4,\\ &|11\rangle_1|11\rangle_2|00\rangle_3|00\rangle_4,\quad |00\rangle_1|00\rangle_2|11\rangle_3|11\rangle_4,\end{aligned} \tag{A8}$$

with the energy equal to $-4V_0$. However, the above ground states can be further gapped out by taking into account the following interactions:

$$H_{1234}=\sum_s(V_{1234}^{(4)}c_{1,s}^\dagger c_{2,s}^\dagger c_{3,s}\ c_{4,s}+V_{1234}^{(4)}c_{1,s}\ c_{2,s}c_{3,s}^\dagger c_{4,s}^\dagger). \tag{A9}$$

In the 4-dimensional Hilbert space spanned by the ground states in Eq. (A8), the above interaction can be written in the matrix form

$$\mathcal{H}_{1234}=V_{1234}^{(4)}\begin{pmatrix}0&0&1&1\\0&0&1&1\\1&1&0&0\\1&1&0&0\end{pmatrix}, \tag{A10}$$

whose eigenvalues are $-2V_{1234}^{(4)},0,0$, and $2V_{1234}^{(4)}$. We therefore obtain the single non-degenerate ground state with the energy $-2|V_{1234}^{(4)}|-4V_0$. This implies that under interaction the 4-chain system can be smoothly connected to a trivial phase without closing the bulk gap, and we therefore complete the proof that the Z classification can be broken down to Z_4 under interactions.

Appendix B: Particle fractionalization

We prove in this section that each edge state leads to 1/2-fractionalization. A convenient way is to consider the semi-infinite geometry which has the open boundary at $x = 0$. We then calculate the particle number of the zero mode localized on this boundary. Note the total number of quantum states in the system is given by

$$N = \sum_{E<0} \langle \psi_E | \hat{n}_E | \psi_E \rangle + \sum_{E>0} \langle \psi_E | \hat{n}_E | \psi_E \rangle + \langle \psi_0 | \hat{n}_E | \psi_0 \rangle, \tag{B1}$$

where we denote by $\hat{n}_E = \mathbb{I}$ the state number operator and $|\psi_E\rangle$ is the eigenstate with energy E. Since the Hamiltonian satisfies $\{\mathcal{H}, \sigma_x\} = 0$, the energy spectrum is symmetric. We have then $\sum_{E<0} \langle \psi_E | \hat{n}_E | \psi_E \rangle = \sum_{E>0} \langle \psi_E | \hat{n}_E | \psi_E \rangle$. It follows that

$$\sum_{E<0} \langle \psi_E | \hat{n}_E | \psi_E \rangle = \frac{1}{2}[N - \langle \psi_0 | \hat{n}_E | \psi_0 \rangle]. \tag{B2}$$

The particle number of the zero mode depends on its occupation. If the zero mode is unoccupied, the particle number of it is given by

$$n_0 = \sum_{E<0} \left[\langle \psi_E | \hat{n}_E | \psi_E \rangle_1 - \langle \psi_E | \hat{n}_E | \psi_E \rangle_0 \right]. \tag{B3}$$

Here $\langle\rangle_1$ and $\langle\rangle_0$ represents the cases with one (topological phase) and zero (trivial phase) bound modes, respectively. Using the Eq. (B2) one finds directly

$$n_0 = -\frac{1}{2} \langle \psi_0 | \hat{n}_E | \psi_0 \rangle = -\frac{1}{2}. \tag{B4}$$

Similarly, if the zero mode is occupied, the particle number is $n_0 = 1/2$. It is trivial to know that this result can be applied to the case with two boundaries located far away from each other, say respectively at $x = 0$ and $x = L$. Since the two zero modes are obtained independently, each of them carries $+1/2$ ($-1/2$) particle if it is occupied (unoccupied).

Appendix C: Derivation of the RG equations

In this section we provide the derivation of the one-loop RG equations. We consider that in Hamiltonian (A1) only one Zeeman term, e.g. Γ_y is nonzero (The case with $\Gamma_z \neq 0$ can be studied in the similar way). We find it convenient to redefine that $\hat{c}_{j\downarrow} \to e^{i\pi x_j/a} \hat{c}_{j\downarrow}$ and rewrite the Hamiltonian (A1) in the form: $H = -t_s \sum_{<i,j>,\sigma} \hat{c}^\dagger_{i\sigma} \hat{c}_{j\sigma} + H_{\mathrm{SO}} + H_{\mathrm{Z}}$, where $H_{\mathrm{SO}} = t^{(0)}_{\mathrm{so}} \sum_j (-1)^j (c^\dagger_{j\uparrow} c_{j+1,\downarrow} - c^\dagger_{j\uparrow} c_{j-1,\downarrow} + \mathrm{h.c.})$ and $H_{\mathrm{Z}} = \Gamma_y \sum_j (-1)^j (i c^\dagger_{j\downarrow} c_{j\uparrow} - \mathrm{h.c.})$. The low-energy physics can be well captured by the continuum approximation ($x = ja$):

$$c_{j\sigma} \approx \sqrt{a}[\psi_{R\sigma}(x) e^{ik_F x} + \psi_{L\sigma}(x) e^{-ik_F x}], \tag{C1}$$

with $k_F = \pi/2$. The continuum representation of the two mass terms are given by:

$$H_{\mathrm{SO}} \approx iu \int dx\, (\psi^\dagger_L \sigma^x \psi_R - \psi^\dagger_R \sigma^x \psi_L), \quad H_{\mathrm{Z}} = w \int dx\, (\psi^\dagger_R \sigma^y \psi_L + \psi^\dagger_L \sigma^y \psi_R). \tag{C2}$$

Here $u = 2t_{\mathrm{so}}, w = \Gamma_y$. Using the standard bosonization formula $\psi_{rs} = \frac{1}{\sqrt{2\pi a}} e^{-\frac{i}{\sqrt{2}}[r\phi_\rho - \theta_\rho + s(r\phi_\sigma - \theta_\sigma)]}$ with $r = R, L$ and $s =\uparrow, \downarrow$, we reach that

$$\mathcal{H}_{\mathrm{SO}} = \frac{u}{\pi a} \sin\sqrt{2}\phi_\rho \cos\sqrt{2}\theta_\sigma, \quad \mathcal{H}_{\mathrm{Z}} = \frac{w}{\pi a} \cos\sqrt{2}\phi_\rho \sin\sqrt{2}\theta_\sigma. \tag{C3}$$

The allowed four-fermion interactions in the (unperturbed) Hubbard model at half-filling is highly constrained by the $\mathbb{SU}(2) \times \mathbb{SU}(2)$ symmetry. It is convinient to define current operators:

$$J_r = \psi^\dagger_{r\alpha} \psi_{r\alpha}, \vec{J}_r = \frac{1}{2} \psi^\dagger_{r\alpha\alpha\beta} \psi_{r\beta}, I_r = \psi_{r\alpha} \epsilon_{\alpha\beta} \psi_{r\beta}. \tag{C4}$$

Here ϵ is the fully anti-symmetric tensor. The general form of four-fermion interaction is given by

$$\mathcal{H}_{\text{int}} = 2g_\sigma \vec{J}_R \cdot \vec{J}_L + \frac{g_\rho}{4}(I_R^\dagger I_L + \text{h.c.}). \tag{C5}$$

We then derive the RG flow equations to understand the fate of the topological phase transition driven by the competition of the staggered Zeeman term and the spin-orbit coupling term. The tree level term can be easily read off from the scaling dimensions of $\mathcal{H}_{\text{SO}}$ and $\mathcal{H}_{\text{Z}}$ in their bosonization form (C3), both of which are $(1+K_\rho)/2$. Thus it is necessary to go to the next order in the perturbative expansion. The one-loop order RG flow can be most easily derived by calculating the operator algebra of the various operators [1, 2].

To derive the RG equation, we consider the partition function in the Euclidean functional integral representation

$$\mathcal{Z} = \int \mathcal{D}\overline{\psi}\mathcal{D}\psi e^{-S}. \tag{C6}$$

The Euclidean action $S = \int dx d\tau\, (\mathcal{H}_0 + \mathcal{H}_1)$ where $\mathcal{H}_0$ is the unperturbed Gaussian part and the $\mathcal{H}_1 = \mathcal{H}_{\text{SO}} + \mathcal{H}_{\text{Z}}$ is the perturbation. To perform the RG, we expand the exponential to the second order in $\mathcal{H}_1$. Let us write $\mathcal{H}_1 = \sum g_i \mathcal{O}_i$. Then the second order term is given by

$$\frac{1}{2} g_i g_j \sum_{i,j} \int_{z,w} \langle \mathcal{O}_i(z)\mathcal{O}_j(w)\rangle \simeq \frac{1}{2} g_i g_j \sum_{i,j} \int_{z,w} \frac{c_{ijk}}{4\pi^2 |z-w|^2}\mathcal{O}_k. \tag{C7}$$

We have introduced complex coordinates z, w where $z = v\tau - ix$. Here we assume the following operator product expansion (OPE)

$$\mathcal{O}_i(z)\mathcal{O}_j(0) \sim \frac{c_{ijk}}{4\pi^2|z|^2}\mathcal{O}_k + \text{regular terms}, \tag{C8}$$

which is sufficient for our purpose. The OPEs are valid when two points z and 0 are brought close together, as replacement within correlation functions.

At this point the cutoff prescription needs to be carefully specified. We will choose a short-distance cutoff a in space, but none in imaginary time. For a rescaling factor b, we must then perform the integral

$$I = \int_{a<|x|<ba} dx \int_{-\infty}^{\infty} d\tau \frac{1}{v^2\tau^2 + x^2} = \frac{2\pi}{v} \ln b. \tag{C9}$$

Eq. (C7) then becomes

$$\frac{c_{ijk}}{4\pi v} g_i g_j \ln b \int \mathcal{O}_k. \tag{C10}$$

Upon re-exponentiating we obtain the one-loop RG equation

$$\frac{dg_k}{dl} = -\frac{1}{4\pi v}\sum_{ij} c_{ijk} g_i g_j. \tag{C11}$$

Here $l = \ln b$.

Now let us be more specifit. Besides the current operators defined in (C), we also need to define

$$M_i = \psi_R^\dagger \sigma^i \psi_L,\ i = x, y. \tag{C12}$$

The fermionic field operators satisfy the following OPEs:

$$\psi_{R\alpha}(z)\psi_{R\beta}^\dagger(0) \sim \frac{\delta_{\alpha\beta}}{2\pi z},\quad \psi_{L\alpha}(z)\psi_{L\beta}^\dagger(0) \sim \frac{\delta_{\alpha\beta}}{2\pi z^*}. \tag{C13}$$

The OPEs of the currents and the mass M_i can be calculated from (C13) using Wick's theorem. Those between the currents are standard and can be found in [2] which we do not duplicate. Below are the needed ones:

$$\begin{aligned} M_i(z)\vec{J}_R \cdot \vec{J}_L(0) &\sim \frac{1}{16\pi^2|z|^2} M_i(z), \quad M_i^\dagger(z)\vec{J}_R \cdot \vec{J}_L(0) \sim \frac{1}{16\pi^2|z|^2} M_i^\dagger(z) \\ M_i(z)[I_R I_L^\dagger + \text{h.c.}](0) &\sim -\frac{2}{4\pi^2|z|^2} M_i^\dagger(z), \quad M_i^\dagger(z)[I_R I_L^\dagger + \text{h.c.}](0) \sim -\frac{2}{4\pi^2|z|^2} M_i(z). \end{aligned} \tag{C14}$$

Applying the above formalism to the model at hand, we find

$$\begin{aligned}\frac{du}{dl}&=\frac{3-K_\rho}{2}u-\frac{g_\rho u}{4\pi v_F}+\frac{g_\sigma u}{4\pi v_F},\\ \frac{dw}{dl}&=\frac{3-K_\rho}{2}w+\frac{g_\rho u}{4\pi v_F}+\frac{g_\sigma u}{4\pi v_F},\\ \frac{dg_\sigma}{dl}&=\frac{1}{\pi v_F}g_\sigma^2,\quad \frac{dg_\rho}{dl}=\frac{1}{\pi v_F}g_\rho^2.\end{aligned} \tag{C15}$$

If we take the interaction in the lattice model to be an on-site Hubbard form: $H_U = U\sum_i n_{i\uparrow}n_{i\downarrow}$, the bare values of the coupling coefficients are

$$g_\rho = U, g_\sigma = -U. \tag{C16}$$

Then for the repulsive interaction $U > 0$, the coupling parameter g_σ of the spin sector is marginally flows to zero, while g_ρ is marginally relevant.

[1] J. Cardy, Scaling and Renormalization in Statistical Physics (Cambridge University Press, 1996)
[2] L. Balents and M. P. A. Fisher, Phys. Rev. B **53**, 12133 (1996).